

# Numerical Study of the Dielectric Omnidirectional Visible Mirror

Abir Mouldi<sup>1, 3, \*</sup>, Hamdi Ayed<sup>2, 3</sup>, Mounir Kanzari<sup>4</sup>, and Khaled M. Khedher<sup>2, 5</sup>

**Abstract**—It is well known that high refractive index contrast is essential to the formation of an omnidirectional Photonic Band Gap (PBG). It is generally cited also that the width of the omnidirectional PBG of a dielectric mirror is determined by the refractive-index contrast. But in this work, we show that this condition is not really general criteria. Dielectric mirror with higher refractive index contrast does not necessarily mean that it has the largest omnidirectional photonic band gap. So, we investigate the necessary conditions on the high and low refractive indices of the quarter wave layers to have the largest omnidirectional bandwidth in the visible range. We present a profound study of the omnidirectional band center wavelength and the bandwidth behaviors versus the layers refraction indices. It is shown therefore that one can modulate omnidirectional photonic band gap center by modulating the optical phase of the mirror.

## 1. INTRODUCTION

Recently, a great deal of effort has been devoted to the study of photonic crystals both theoretically and experimentally. Photonic crystals are photonic band gap materials which are known to forbid the propagation of incident electromagnetic waves within a frequency spectrum. They have attracted much attention due to promising applications in optical devices such as waveguides, cavities, mirrors, optical switches, and antireflexion coating [1, 2]. Many studies are focused on the fabrication of omnidirectional mirror which is a photonic crystal able to reflect a range of frequencies for any angle and any polarization. Metallic mirrors are the most common mirrors and reflect strongly for both TE and TM polarizations from normal incidence to grazing angles. However, in the infrared and optical region, metals are highly absorptive. Unlike their metallic counterparts, dielectric mirrors absorb very little incident light energy [3, 4]. Until recently, the design of a complete photonic band gap was associated with three-dimensional photonic crystal which is a complicated structure. Fink et al. [5] have reported that one-dimensional photonic crystal possesses the feature of omnidirectional reflection for all the polarizations and angles of incidence. The mirror was fabricated as a quarter-wave stack of the polystyrene (as low refractive index of 1.6) and tellurium (as high refractive index of 4.6) films in 10–15  $\mu\text{m}$  of the infrared spectrum. Therefore, this novel property furnishes a wide platform for practical applications based on a multilayer structure.

It is well known that high refractive-index contrast is essential to the formation of large PBGs [6–8]. However, in visible range, the choice of the optical contrast ratio is not evident since we are limited by the dielectrics existing and having a low absorption in the visible. Most materials in the visible have low refractive index value [6, 7]. But nowadays, some techniques are investigated to have materials with desired refractive index. For example, Bananej et al. [9] propose a flexible design for one-dimensional photonic crystals in which the low index layers are replaced by equivalent three-layers which consist

---

*Received 13 February 2020, Accepted 14 April 2020, Scheduled 23 April 2020*

\* Corresponding author: Abir Mouldi (amouldi@kku.edu.sa).

<sup>1</sup> Department of Industrial Engineering, College of Engineering, King Khalid University, Abha 61421, KSA. <sup>2</sup> Department of Civil Engineering, College of Engineering, King Khalid University, Abha 61421, KSA. <sup>3</sup> Higher Institute of Transport and Logistics, Sousse University, Cité Erriadh, BP 247 Sousse 4023, Tunisia. <sup>4</sup> National Engineers School of Tunis, BP 37 le Belvédère 1002, Tunisia.

<sup>5</sup> Department of Civil Engineering, ISET, Nabeul, DGSET, Tunisia.

of the same applicable and compatible materials of the basic structure but with different fractional optical thicknesses. So the effective optical contrast ratio is adjusted by this technique. Refractive index can also be adjusted by imposing some temperature because the permittivity and permeability of materials are related to temperature [10]. Furthermore, illumination by an intense laser beam can produce small (nonlinear) changes in the refractive index of a constitutive material of the photonic crystal [11]. Deopura et al. [6] demonstrate the fabrication of a dielectric omnidirectional mirror for visible frequencies. The dielectric reflector consists of a stack of 19 alternating layers of tin (IV) sulfide and silica.

It is generally cited that the width of the omnidirectional PBG of a dielectric mirror is determined by the refractive-index contrast [12,13]. But in this work, we show that this condition is not really general criteria. Dielectric mirror with higher refractive index contrast does not necessarily mean that it has the largest omnidirectional PBG. So, we investigate the suitable choice of the high and low refractive indices of the quarter wave layers to have the largest omnidirectional bandwidth in the visible range. Then, we study the effect of the high and low refractive indices on the omnidirectional PBG center. Southwell [14] has given analytical approximations for an omnidirectional mirror consisting of a quarter-wave dielectric stack. Leckner [15] has improved these analytical approximations. In this work, we give numerical approximations using computer simulations calculated through numerical modeling by the transfer matrix method. Understanding of such an effect is of great importance since it would be useful for the design and fabrication of omnidirectional mirrors in the visible spectrum. Then, we propose to modulate the center of the omnidirectional PBG using the approach of chirping.

## 2. METHOD OF MODELING

For the calculation of system reflection and transmission, we employ the Transfer Matrix Method (TMM). This technique is a finite difference method particularly well suited for the study of the scattering (transmission, reflection, and absorption) spectrum [16]. It is based on Abelès method [17] in terms of forward and backward propagating electric fields, that is,  $E^+$  and  $E^-$  which were introduced to calculate the reflection and transmission. Abelès showed that the relation between the amplitudes of the electric fields of the incident wave  $E_0^+$ , reflected wave  $E_0^-$ , and transmitted wave after  $m$  layers,  $E_{m+1}^+$ , is expressed as the following matrix for stratified films within  $m$  layers:

$$\begin{pmatrix} E_0^+ \\ E_0^- \end{pmatrix} = \frac{C_1 C_2 C_3 \dots C_{m+1}}{t_1 t_2 t_3 \dots t_{m+1}} \begin{pmatrix} E_{m+1}^+ \\ E_{m+1}^- \end{pmatrix} \quad (1)$$

Here,  $C_j$  is the propagation matrix with the matrix elements.

$$C_j = \begin{pmatrix} \exp(i\phi_{j-1}) & r_j \exp(-i\phi_{j-1}) \\ r_j \exp(i\phi_{j-1}) & \exp(-i\phi_{j-1}) \end{pmatrix} \quad (2)$$

where  $t_j$  and  $r_j$  are the Fresnel transmission and reflection coefficients, respectively, between the  $(j-1)^{th}$  and  $j^{th}$  layers. The Fresnel coefficients  $t_j$  and  $r_j$  can be expressed as follows by using the complex refractive index  $\hat{n}_j = n_j + ik_j$  and complex refractive angle  $\theta_j$ . For Transverse Magnetic (TM) polarization (Parallel polarization):

$$r_{j\text{TM}} = \frac{\hat{n}_{j-1} \cos \theta_j - \hat{n}_j \cos \theta_{j-1}}{\hat{n}_{j-1} \cos \theta_j + \hat{n}_j \cos \theta_{j-1}} \quad (3)$$

$$t_{j\text{TM}} = \frac{2\hat{n}_{j-1} \cos \theta_{j-1}}{\hat{n}_{j-1} \cos \theta_j + \hat{n}_j \cos \theta_{j-1}} \quad (4)$$

Moreover, for Transverse Electric (TE) polarization (Perpendicular polarization):

$$r_{j\text{TE}} = \frac{\hat{n}_{j-1} \cos \theta_{j-1} - \hat{n}_j \cos \theta_j}{\hat{n}_{j-1} \cos \theta_{j-1} + \hat{n}_j \cos \theta_j} \quad (5)$$

$$t_{j\text{TE}} = 2 \frac{\hat{n}_{j-1} \cos \theta_{j-1}}{\hat{n}_{j-1} \cos \theta_{j-1} + \hat{n}_j \cos \theta_j} \quad (6)$$

The complex refractive indices and complex angles of incidence obviously follow Snell's law:  $\hat{n}_{j-1} \sin \theta_{j-1} = \hat{n}_j \sin \theta_j$  ( $j = 1, 2 \dots m + 1$ ). The values  $\phi_{j-1}$  in Equation (2) indicate the change in the phase of the wave between the  $(j - 1)$ th and  $j$ th boundaries and are expressed by the equation:

$$\phi_0 = 0 \tag{7}$$

$$\phi_{j-1} = \frac{2\pi}{\lambda} \hat{n}_{j-1} d_{j-1} \cos \theta_{j-1} \tag{8}$$

Except for  $j = 1$ ,  $\lambda$  is the wavelength of the incident light in vacuum, and  $d_{j-1}$  is the thickness of the  $(j - 1)$ th layer. By putting  $E_{m+1}^- = 1$ , because there is no reflection from the final phase, Abele's obtained a convenient formula for the total reflection and transmission coefficients, which correspond to the amplitude reflectance  $r$  and transmittance  $t$ , respectively, as follows:

$$r = \frac{E_0^-}{E_0^+} = \frac{c}{a} \tag{9}$$

$$t = \frac{E_{m+1}^+}{E_0^+} = \frac{t_1 t_2 \dots t_{m+1}}{a} \tag{10}$$

Quantities  $a$  and  $c$  are the matrix elements of the all product  $C_j$  matrix:

$$C_1 C_2 C_3 \dots C_{m+1} = \begin{pmatrix} a & b \\ c & d \end{pmatrix} \tag{11}$$

By using Equations (9) and (10), we can easily obtain the energy reflectance  $R$  as:

$$R = |r|^2 \tag{12}$$

For (TM) and (TE) polarizations and the energy transmittance  $T$ :

$$T_{TE} = \text{Re} \left( \frac{\hat{n}_{m+1} \cos \theta_{m+1}}{\hat{n}_0 \cos \theta_0} \right) |t_{TE}|^2 \tag{13}$$

$$T_{TM} = \text{Re} \left( \frac{\cos \theta_{m+1} / \hat{n}_{m+1}}{\cos \theta_0 / \hat{n}_0} \right) \left| \frac{\hat{n}_{m+1}}{\hat{n}_0} t_{TE} \right|^2 = \text{Re} \left( \frac{\hat{n}_{m+1} \cos \theta_{m+1}}{\hat{n}_0 \cos \theta_0} \right) |t_{TM}|^2 \tag{14}$$

for TE and TM polarization, respectively, where Re indicates the real part.

### 3. RESULTS AND DISCUSSIONS

#### 3.1. Study of the Omnidirectional PBG of the Quarter Wavelength Mirror

For the numerical computations, we consider a typical system based on a one-dimensional perfectly periodic structure consisting of two alternating dielectric layers  $H(LH)^j$ .  $H$  is the high refractive index material, and  $L$  is the low one.  $j$  is the period's number, which is chosen as 15. Layers are quarter wavelength where the reference wavelength value is  $0.5 \mu\text{m}$ , the middle of the visible spectrum. Glass with refractive index  $n_S = 1.5$  is the substrate, and ambient medium is air with  $n_a = 1.0$ . In order to achieve omnidirectional reflectivity, we must require that the zero transmission bands have a common overlapping region for all incidence angles and for both polarizations. A necessary condition for omnidirectional PBG for both polarizations is that the maximum angle of refraction  $\theta_{H,Max}$  inside the first layer is less than the Brewster angle  $\theta_B$  of the second interface so that the Brewster angle can never be accessed by a wave incident on the first interface. If this condition is not satisfied, a Transverse Magnetic (TM) wave would not be reflected at the second and all subsequent interfaces and will transmit through the structure. Brewster's angle exists only for TM waves and is determined by the ratio of the refractive indices of two materials in the periodic structure. So the formation of the omnidirectional PBG is determined by this ratio.

It is always reported that its width is also determined by this ratio. It means that the system with the higher refraction index contrast has a larger omnidirectional PBG. To illustrate that this fact is not really general criteria, we can investigate the behavior of a first structure (1) which has as

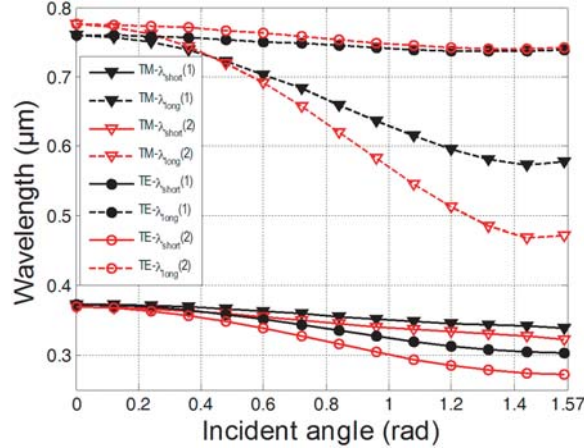


**Figure 1.** Photonic band gap shift as a function of incident angle for TM and TE polarizations for the two studied structure (1) (black plots) and (2) (red plots). Solid lines represent the lower photonic band edges; dashed lines represent the upper photonic band edges. Triangular markers represent TM polarization, Circular ones represent TE polarization.

high and low refractive indices respectively  $n_H = 4.6$  and  $n_L = 1.45$  and that of a second structure (2) where  $n_H = 4$  and  $n_L = 1.2$  with all the other parameters kept the same. We can observe this behavior through diagram bands of the two structures shown in Figure 1 which gives the calculated variations of the photonic band gap edges as the function of the incident angle for the two modes of polarization. We define the band gap as the wavelength range when the transmission is less than 0.01%. The omnidirectional PBG for both TE and TM polarizations can be defined by the edges of the upper photonic band at the incident angle of  $90^\circ$  and the lower photonic band at the normal incidence.

For normal incidence, the transmission spectra of TE and TM polarizations degenerate. Therefore, at a high incident angle the reflectance of TM-polarized light is low in contrast to the high reflectance of TE-polarized light. So, the omnidirectional PBGs for the TM polarization are completely located within that for the TE polarization, and then the omnidirectional PBG for any polarization is the omnidirectional PBG for the TM polarization.

It is obvious that the refraction index contrast ratio of the second structure is higher than that of the first one; however, simulations show that the omnidirectional PBG of the first structure is larger than that of the second one. This fact is clear when we examine Figure 1 where we note that the forbidden band under TE polarization of the second structure from normal to grazing angle is wider than that of the first one. Under TM polarization, at normal incidence, the lower edge of the photonic band is the same in the two structures, but the upper edge of the second one is higher, and its band is still wider for angles below  $26^\circ$  (0.46 rad). Above this angle, the upper edge of the first structure becomes higher than that of the second one, and as the angle increases the difference between the two edges increases pronouncedly. As a result, the omnidirectional PBG of structure (1) is broader than that of structure (2). Consequently, it is convenient to study the variation of the omnidirectional bandwidth as a function of  $n_H$  and  $n_L$ . For this, we display a curve (Figure 2) which represents the omnidirectional PBG width as a function of  $n_H$  and  $n_L$ . Since the system omnidirectional PBG is the omnidirectional PBG for the TM polarization, it is sufficient to calculate the omnidirectional bandwidth under TM polarization to plot the curve. The plane surface represents the couples of  $n_H$  and  $n_L$  for which there is no omnidirectional PBG.

The curve shows that the high refractive index should be larger than 2.6 to have an omnidirectional PBG. At given  $n_L$ , the increase of  $n_H$  produces an increase of the omnidirectional bandwidth. Figure 3(a) shows in 2D the variation of the omnidirectional bandwidth as a function of  $n_H$  for different values of  $n_L$ . The minimum value of the necessary  $n_H$  to have an omnidirectional reflection differs according to  $n_L$ . Figure 4(a) displays the variation of the required high refraction index for getting omnidirectional reflection for each  $n_L$ . The parabolic form of the curve exhibits the opportunities to obtain an omnidirectional reflection for different materials according to their refraction indices. It is

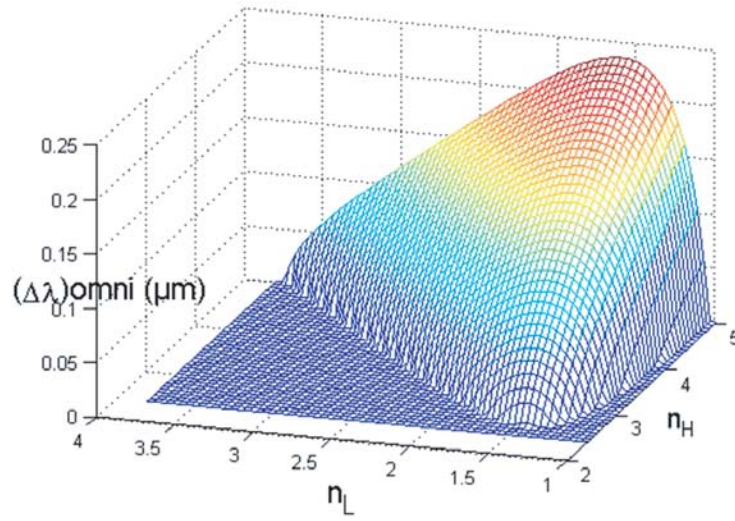


**Figure 2.** Omnidirectional photonic bandwidth as a function of the high and low refractive indices.

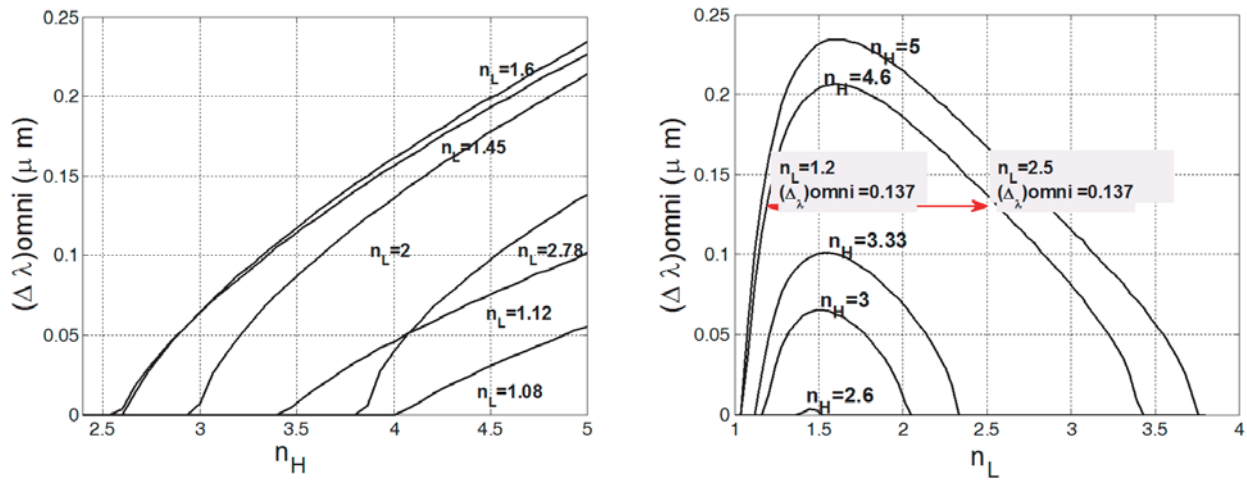


**Figure 3.** Omnidirectional photonic bandwidth as function of (a) high refractive index for different low refractive indices (b) low refractive index for different high refractive indices.

obvious that in the visible range, this opportunity is more pronounced for  $n_L$  which is between 1.2 and 2.2, and  $n_H$  is between 2.6 and 3.3 in view of the fact that most materials have low refraction index in the visible frequency range.

For a better understanding of the performance of the structure, we calculate the required refraction index contrast for getting omnidirectional reflection for each  $n_L$ . Figure 4(b) displays the required contrast as a function of  $n_L$ . We note that the required contrast differs also according to  $n_L$ . For low values of  $n_L$ , a very high contrast is necessary to have an omnidirectional PBG; however, the descending tendency of the curve shows that the required contrast decreases with higher low refraction index. The descending variation is more important for lower values of  $n_L$ .

In Figure 3(b), the omnidirectional bandwidth is plotted in terms of the low refraction index for different values of  $n_H$ . From the plots, it is observed that initially omnidirectional bandwidth is zero below a certain value of  $n_L$  (which differs according to  $n_H$ ), then it increases pronouncedly with increasing  $n_L$  to a maximum value, and subsequently it is almost constant through a narrow interval, while then it decreases slowly with  $n_L$ , and finally it again comes to zero at some value of  $n_L$  above which

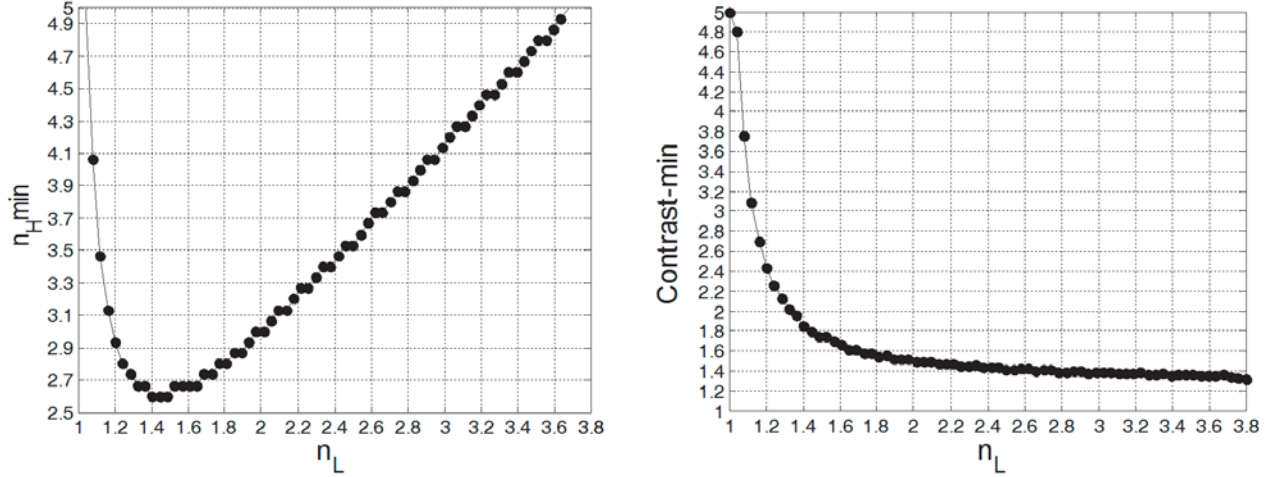


**Figure 4.** Variation of the lowest required (a) high refractive index (b) refractive index contrast ratio to have omnidirectional reflection as function of the low refractive index.

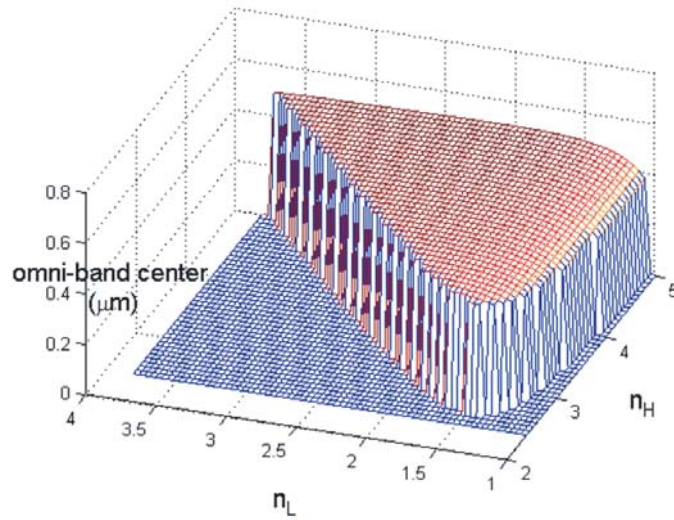


**Figure 5.** Omnidirectional photonic band gap center as function of the high and low refractive indices.

no omnidirectional bandwidth is obtained. The maximum omnidirectional bandwidth is obtained at the value of  $n_L$  between 1.45 and 1.65. The bell shape of the curve shows that at specified high refractive index, and there are two values of low refractive index for the same value of bandwidth. For example, at  $n_H = 4.6$ , we can have a bandwidth of  $0.137 \mu m$  with  $n_L = 1.2$  or  $n_L = 2.5$ .

As a general feature, we note that the air with refractive index  $n = 1$  is not suitable as low refractive index material in the visible range. Through this analysis, we are able to explain the results of simulations shown in Figure 1. Firstly, the high refractive index of the first structure is higher than that of the second structure, and secondly, the low refractive index of the first structure belongs to the optimal interval of  $n_L$ .

The dependence of central wavelength of the omnidirectional PBG on the refractive indices  $n_H$  and  $n_L$  is shown in Figure 5. The red part presents the region where we have an omnidirectional reflection. To examine carefully the behavior of the omni-band center versus  $n_H$  and  $n_L$  variation, we plot Figures 6(a) and 6(b). As shown in Figure 6(a), the central wavelength increases with the rise of  $n_H$ . But we note also that in all cases, the wavelength center is lower than  $0.5 \mu m$  which is the reference wavelength. For lower values of  $n_L$ , the omnidirectional band is centered at short wavelength. For example, when we

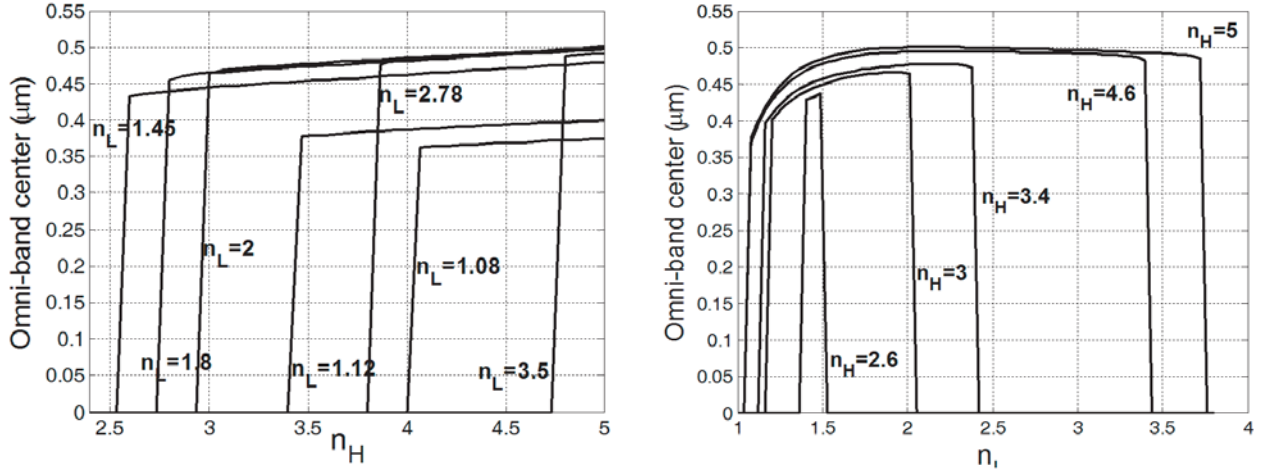


**Figure 6.** Omnidirectional photonic band gap center as function of (a) high refractive index for different low refractive indices (b) low refractive index for different high refractive indices.

have  $n_L = 1.08$ , the highest omnidirectional band center that we can obtain when  $n_H$  varies between 2.4 and 5 is  $0.37 \mu\text{m}$ . The omnidirectional band center shifts to longer wavelength when  $n_L$  increases. This is noted also in Figure 6(b) which gives the variation of the omnidirectional band center as a function of  $n_L$  for different values of  $n_H$ . The omnidirectional band center increases with the increase of  $n_L$ , but at the end of each curve, it decreases through a small interval to fall finally to zero value where there is no omnidirectional reflection.

### 3.2. Modulation of the Omnidirectional PBG Center

We have extended the mathematically rigorous transfer matrix method to calculate the light propagation in chirped mirror. The use of a chirped mirror instead of a uniform period one offers the benefit of a larger bandwidth [18]. Several researches on chirped mirrors have been reported, and the purpose is always the widening of the photonic band gap [19, 20]. In this work, we propose to introduce chirping to tune the center of the omnidirectional PBG. We conclude in the last part that the quarter wave mirror has an omnidirectional bandgap center below the reference wavelength whatever the values of the high and low refraction indices. So we look for a chirping form which generates a shift of the omnidirectional band gap center without causing a great enlargement of the omnidirectional bandwidth. For this, we impose on the structure a chirping by applying a power law, so that the coordinates  $y$  which represents the transformed object are determined using the coordinates  $x$  of the initial object in accordance with the rule:

$$y = x^{k+1} \tag{15}$$

where  $k$  is the chirping degree. This implies that the optical phase thickness of the  $j^{th}$  layer is:

$$\phi_j = \frac{2\pi}{\lambda} \frac{\lambda_0}{4} [j^{k+1} - (j-1)^{k+1}] \cos\theta_j, \tag{16}$$

The initial optical phase thickness is:

$$\phi = \frac{2\pi}{\lambda} \frac{\lambda_0}{4} \cos\theta. \tag{17}$$

For the chirped system, the optical thickness of each layer becomes variable and depends on the  $j^{th}$  layer and chirping degree  $k$ . So, the optical thickness of each layer after deformation by the  $y$  function takes the following form:

$$x(j) = \frac{\lambda_0}{4} [j^{k+1} - (j-1)^{k+1}] \tag{18}$$

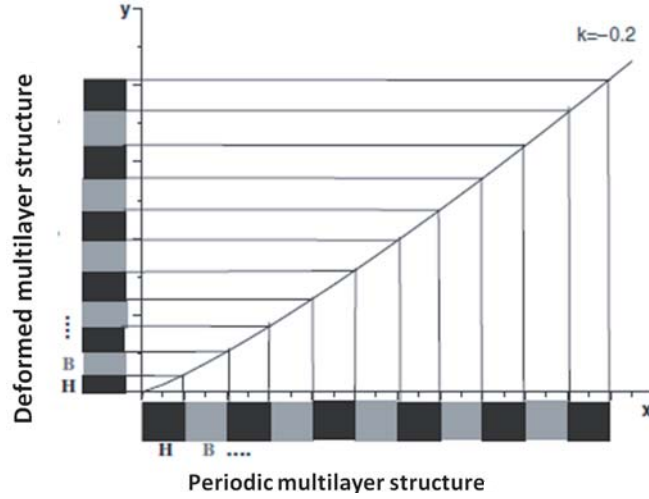


**Figure 7.** Principle of introducing the chirping into a periodic multilayer structure, for example for  $k = -0.2$ .

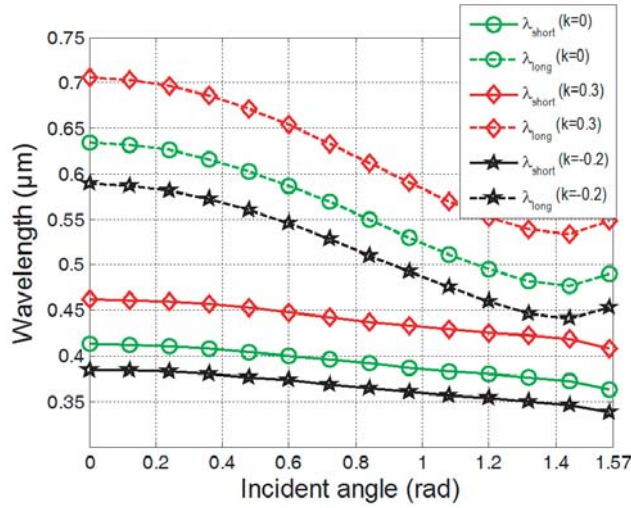


**Figure 8.** Photonic band gap shift as a function of incident angle for TM polarization of the quarter wave structure and the chirped structure.

Figure 7 describes the principle of the transformed system by the  $y$  function. We apply this form of chirping because compared with the other forms used in literature, this rule generates a fast shifting of the bandgap center wavelength without a significant enlargement of the bandwidth. To prove this, we consider a structure with high and low refractive indices which are taken to be  $n_H = 3$  and  $n_L = 1.45$ . We display the shifting of the PBG edges under TM polarization of three cases; the perfectly quarter wave periodic photonic crystal, the chirped one with  $k$  chosen  $-0.2$ , and then  $k$  is chosen to be  $0.3$  (Figure 8). At each incident angle, the lower and upper edges of the forbidden PBG of the chirped structure shift to the longer wavelengths when  $k = 0.3$  and to the shorter wavelengths when  $k = -0.2$ . Table 1 gives the omnidirectional PBG properties for some values of  $k$ . It is obvious that for negative values of  $k$ , the displacement of the omnidirectional PBG center is toward shorter wavelengths; however, for positive values of  $k$ , the displacement is toward the longer wavelengths. Consequently, the omnidirectional PBG center is tunable by the choice of parameter  $k$ .

To coincide the omnidirectional PBG center exactly with the reference wavelength which is  $0.5 \mu\text{m}$ , we choose  $k = 0.31$ . Among many possible applications, a tunable photonic band gap allows a modulation, or at least a fine control of the photonic properties.

**Table 1.** The omnidirectional PBG properties for different values of chirping degree  $k$ .

$k$	-0.07	-0.031	-0.01	.01	0.031	0.07
$\lambda_{omni_{center}}$ ( $\mu\text{m}$ )	0,041	0,0504	0,059	0,063	0,067	0,077
$\Delta\lambda_{omni}$ ( $\mu\text{m}$ )	0,340	0,396	0,428	0,444	0,462	0,578

#### 4. CONCLUSION

Since the refraction index contrast is an obligatory but not a sufficient condition to have a large omnidirectional photonic band gap, we have analyzed the variation of the omnidirectional bandwidth as a function of the high and low refraction indices variation using the transfer matrix method for the calculation of the omnidirectional photonic band gap. We have derived that the high refractive index should be larger than 2.6 for the design of an omnidirectional dielectric mirror. Then, at fixed  $n_L$ , omnidirectional bandgap increases with increasing  $n_H$ , and at fixed  $n_H$ , omnidirectional bandgap increases with increasing  $n_L$ , which reaches its maximum and then decreases. The low refractive index should be between 1.45 and 1.65 for the maximum omnidirectional bandwidth. The dependence of the central wavelength on the high and low refractive indices is also studied. The results reveal that the omnidirectional bandgap center is generally lower than the reference wavelength, so with the quarter wave stack, the omnidirectional PBG is not necessarily centered on the reference wavelength. So, we propose to introduce the chirping into the structure to modulate the bandgap center and coincide it with the reference wavelength.

#### ACKNOWLEDGMENT

This study was financially supported by the Deanship of Scientific Research at King Khalid University (Grant number R.G.P. 2/56/40).

#### REFERENCES

1. Li, Z.-Y., "Principles of the plane-wave transfer-matrix method for photonic crystals," *Science and Technology of Advanced Materials*, Vol. 6, 837–841, 2005.
2. Mouldi, A. and M. Kanzari, "Broad multilayer antireflection coating by apodized and chirped photonic crystal," *Optics Communications*, Vol. 284, 4124–4128, 2011.
3. Qiang, H., L. Jiang, and X. Li, "Design of broad omnidirectional total reflectors based on one-dimensional dielectric and magnetic photonic crystals," *Optics & Laser Technology*, Vol. 42, 105–109, 2010.
4. Srivastava, R. and S. P. Ojha, "Enhancement of omnidirectional Reflection bands in one-dimensional photonic crystals with left-handed materials," *Progress In Electromagnetics Research*, Vol. 68, 91–111, 2007.
5. Fink, Y., J. N. Winn, S. Fan, C. Chen, J. Michel, J. D. Joannopoulos, and E. L. Thomas, "A dielectric omnidirectional reflector," *Science*, Vol. 282, 1679–1682, 1998.
6. Deopura, M., C. K. Ullal, B. Temelkuran, and Y. Fink, "Dielectric omnidirectional visible reflector," *Opt. Lett.*, Vol. 26, 1197–1199, 2001.
7. Han, P. and H. Wang, "Extension of omnidirectional reflection range in one-dimensional photonic crystals with a staggered structure," *J. Opt. Soc. Am. B*, Vol. 20, 1996–2001, 2003.
8. Joannopoulos, J. D., S. G. Johnson, J. N. Winn, and R. D. Meade, *Molding the Flow of Light*, 2nd Edition, 2007.
9. Bananej, A., S. M. Hamidi, W. Li, C. Li, and M. M. Tehrani, "A flexible design for one-dimensional photonic crystals with controllable photonic bandgap width," *Optical Materials*, Vol. 30, No. 12, 1822–1827, 2008.

10. Sang, Z. F. and Z. Y. Li, "Optical properties of one-dimensional photonic crystals containing graded material," *Optics Communications*, Vol. 259, 174–178, 2006.
11. Galindo-Linares, E., P. Halevia, and A. S. Sanchez, "Tuning of one-dimensional Si/SiO<sub>2</sub> photonic crystals at the wavelength of 1.54  $\mu\text{m}$ ," *Solid State Communications*, Vol. 142, 67–70, 2007.
12. Singh, S. K., J. P. Pandey, K. B. Thapa, and S. P. Ojha, "Structural parameters in the formation of omnidirectional high reflectors," *Progress In Electromagnetics Research*, Vol. 70, 53–78, 2007.
13. Wang, Z. and D. Liu, "A few points on omnidirectional band gaps in one-dimensional photonic crystals," *Appl. Phys. B*, Vol. 86, 473–476, 2007.
14. Southwell, W. H., "Omnidirectional mirror design with quarter-wave dielectric stacks," *Appl. Opt.*, Vol. 38, 5464–5467, 1999.
15. Lekner, J., "Omnidirectional reflection by multilayer dielectric mirrors," *J. Opt. A: Pure Appl. Opt.*, Vol. 2, 349–352, 2000.
16. Li, Z., "Principles of the plane-wave transfer-matrix method for photonic crystals," *Science and Technology of Advanced Materials*, Vol. 6, 837–841, 2005.
17. Abelès, F., *Ann Phys. Paris*, Vol. 12, 596, 1950.
18. Tehranchi, A. and R. Kashyap, "Novel step-chirped quasi-phase matched gratings for broadband frequency doublers with high-efficiency flat response in nonlinear optical waveguides," *19th General Assembly*, 47–51, Chicago, USA, August 7–16, 2008.
19. Bi, G. and H. Wang, "A theoretical study of the chirped and apodized photonic crystals," *PIERS Proceedings*, 571–574, Hangzhou, China, August 22–26, 2005.
20. Mouldi, A. and M. Kanzari, "Design of an omnidirectional mirror using one dimensional photonic crystal with graded geometric layers thicknesses," *OPTIK*, Vol. 123, 125–131, 2012.